PHYSICAL REVIEW B 76, 195402 (2007)

Midinfrared optical response and thermal emission from plasmonic lattices on Al films

Mohit Diwekar,[1] Tatsunosuke Matsui,[1,*] Amit Agrawal,[2] Ajay Nahata,[2] and Z. Valy Vardeny[1,†]
[1]*Department of Physics, University of Utah, Salt Lake City, Utah 84112, USA*
[2]*Department of Electrical and Computer Engineering, University of Utah, Salt Lake City, Utah 84112, USA*
(Received 27 July 2007; revised manuscript received 7 October 2007; published 2 November 2007)

We studied the midinfrared optical transmission and thermal light emission spectra of subwavelength hole arrays in the form of square lattice with 4 μm periodicity (plasmonic lattice) in aluminum films deposited on silicon substrates. The optical transmission of these films showed temperature independent resonance bands and antiresonance dips in the midinfrared spectral range, which could be explained by a model involving light coupling to surface plasmon polaritons (SPPs) on the two film interfaces. We fitted the transmission spectrum using a dielectric response function that is based on an effective plasma frequency determined by the individual holes and resonant modes associated with the reciprocal vectors in the lattice structure factor; subsequently, we also calculated the absorption spectrum. We found that the absorption spectrum shows bands opposite in phase compared to those in the transmission spectrum, where peaks are replaced by dips and vice versa. The thermal emissivity spectrum of the heated perforated films were measured at elevated temperatures and showed resonant bands similar to those in the transmission spectrum rather than the absorption spectrum, in *apparent* contradiction to Kirchhoff's law of radiation. We thus conclude that the perforated films act primarily as radiation filters, where thermal emission is suppressed for frequencies outside the resonant transmission bands. This optical filtering is characteristic of *weak* photonic crystals, where the photon density of states in the heated metal film is only weakly modified by the perforated interfaces, suggesting weak interaction between the SPP excitations on the metal/dielectric interfaces and the photonic states inside the metal film.

DOI: 10.1103/PhysRevB.76.195402 PACS number(s): 73.20.Mf, 42.70.Qs, 42.79.Ag, 42.79.Dj

I. INTRODUCTION

On a smooth metal/dielectric interface, light does not couple to surface plasmon polaritons (SPPs), which are the elementary excitations of the metal surface, because conservation of energy E and momentum $\mathbf{k}$ cannot be simultaneously obeyed.[1] On an $(E,\mathbf{k})$ plot, the SPP dispersion curve lies below that of electromagnetic waves in vacuum. However, in a metallic film that is perforated with two-dimensional (2D) periodic array of holes that forms a 2D metallodielectric photonic crystal, the periodicity allows for grating coupling of the SPP to light that results in resonantly enhanced transmission bands, also referred to as "anomalous transmission" or "extraordinary optical transmission" (EOT). The EOT phenomenon was discovered approximately a decade ago in the ground-breaking work by Ebbesen *et al.*, where the optical transmission through a perforated aluminum (Al) film in the visible and/or near-infrared spectral range was measured.[2] This work launched a large number of experimental and theoretical studies on perforated metal films with subwavelength hole arrays (also known as "plasmonic lattices") having periodic,[2–19] aperiodic,[20–24] and fractal[25] structures. The intense interest in the EOT phenomenon is partially due to potential wide-ranging applications in near-field microscopy,[26] optoelectronics,[27,28] and biosensing.[29] Most of the experimental work to date has dealt with EOT in the visible and/or near-infrared and terahertz spectral ranges. It has been recognized[14,22] that the resonant transmission bands have different properties in these two spectral ranges since the SPP attenuation is much larger in the visible. However, relatively few EOT studies have been performed in the midinfrared (MIR) spectral range.[15,30] The MIR range is particularly interesting since the SPP attenuation is still low in this range, and also commonly available MIR spectrometers may be still used rather than the sophisticated experimental tools needed for the terahertz range measurements.

At approximately the same time of the discovery of EOT through plasmonic lattices, it was suggested that thermal emission radiation from a metallic array should be very different from the well-known Planck blackbody emission spectrum.[31] Specifically, the emission spectrum was calculated to be strongly affected by resonances in the optical spectra. This work has initiated a number of investigations aimed at studying the modification of the thermal emission spectrum from three-dimensional (3D) metallic photonic crystals,[32–41] where strong changes in the emission spectrum compared to metals have been indeed observed. Also, a controversy was recently noticed, where the claim that the thermal emission efficiency of 3D metallic photonic crystals is larger than that of a blackbody was challenged.[39,40] So far, most of the studies of thermal emission from photonic structures have been performed using 3D photonic crystals.[31–41] However, 2D photonic crystals might also change the photonic density of states (DOS) of the heated metals and thus alter the thermal emission spectrum. In particular, it is not clear whether perforated metallic films in the form of a 2D plasmonic lattice that show EOT are sufficiently strong photonic crystals that their thermal emission spectrum is modified.

In this work, we report our study of the optical transmission and thermal emission spectra from plasmonic lattices of hole arrays in square lattice with 4 μm periodicity fabricated in aluminum (Al) optically thick films deposited on silicon substrates. We found the existence of EOT resonances and antiresonances in the MIR spectral range, which can be well explained by a model involving light coupling to SPP exci-

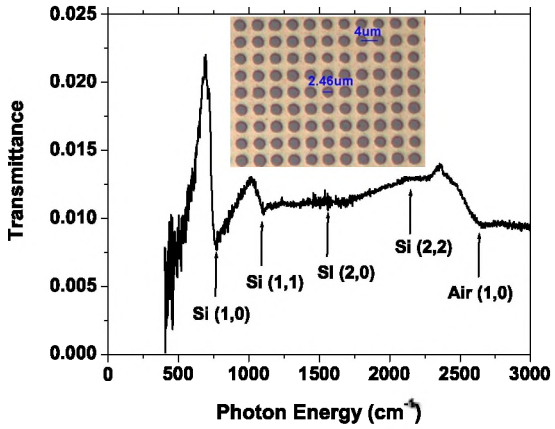

FIG. 1. (Color online) The optical transmission spectrum of an Al hole array (plasmonic lattice) at normal incidence. The arrows and labeled indices represent the surface plasmon modes associated with the different dielectric interfaces of the plasmonic lattice, namely, the substrate (Si) and air, respectively; the frequencies are given in Table I. The inset shows an optical microscope image of the plasmonic lattice sample, where the lattice constant a (=4 μm) and aperture diameter D (=2.46 μm) are assigned.

tations. From the EOT spectrum, we calculated the effective dielectric function and the corresponding absorption spectrum of the perforated metal films using a recently suggested model.[42,43] In this model, the individual holes determine the effective plasma frequency, whereas the lattice structure factor determines the resonant modes associated with the reciprocal vectors.[43] We found that the absorption spectrum of the perforated films exhibits the inverse optical activity of the transmission spectrum; namely, absorption peaks (dips) replace transmission dips (peaks) in the spectrum. Also, the thermal emission from the perforated films is modified compared to that of an unpatterned film. Although the obtained changes in the emissivity spectrum are small, the overall thermal emission spectrum is still strongly altered, primarily because the hole array acts as a radiation filter where the emission is suppressed outside of the resonant EOT bands. This optical filtering is characteristic of *weak* photonic crystals,[44] where the photon DOS in the heated metal film is weakly modified by the perforated interfaces, suggesting weak coupling between the SPP excitations on the metal/dielectric interfaces and the MIR photonic states inside the metal film.

II. EXPERIMENT

Optically thick Al films of ~300 nm were deposited on Si substrates using an e-beam evaporator. The hole array structures with square lattice symmetry were then fabricated using standard photolithographic processes. After patterning the photoresist, the periodic hole array pattern was transferred onto the underlying metal films by a reactive ion-etching method. The hole array lattice constant was 4 μm with a hole diameter of 2.46 μm (Fig. 1, inset). The optical transmission spectrum $T(\omega)$ in the MIR spectral range was measured through the hole arrays at normal incidence using a

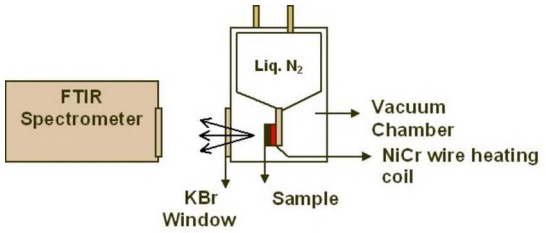

FIG. 2. (Color online) (a) Schematic diagram of the thermal emission measurement setup. The sample is mounted on a NiCr wire heating coil and placed in a vacuum chamber supported by a long ceramic post that is connected to a liquid-nitrogen-cooled cold stage and heated to a temperature of about 600 K during the measurement. The thermal emission spectrum is measured via an external port of a FTIR spectrometer.

Fourier transform infrared spectrometer (FTIR) and subsequently normalized by the transmission spectrum of a bare Si substrate. Since the Al films were opaque in the MIR spectral range, then the obtained EOT bands are due to transmission through the individual holes in relation with interference resonances from the light induced SPP,[2] or other surface waves[14] that are launched[14] on the two Al film interfaces.

The experimental setup for measuring the thermal emission spectra from the heated metallic films was properly configured to minimizing background emission that could have interfered with the main thermal emission spectrum from the sample (Fig. 2). This was achieved by mounting the samples in a liquid nitrogen cooled vacuum chamber that was pumped down to approximately 10^{-5} Torr. The sample was mounted on a NiCr wire heating coil and subsequently heated to $T \sim 600$ K. The thermal emission radiation passed through a KBr cryostat window, and was fed into an external port of the FTIR spectrometer for spectral analysis. A KBr beam-splitter and a DTGS-MIR photodetector were used for the MIR signal detection. This photodetector/beam-splitter combination has a fairly flat spectral response in the MIR spectral range from 3 to 20 μm.

III. RESULTS AND DISCUSSION

A. Extraordinary transmission spectra

As seen in Fig. 1, the transmission spectrum $T(\omega)$ from the perforated films contains a broad enhanced transmission band starting from ~400 cm^{-1}, as well as several resonant EOT bands (indexed from 1 to 5), each followed by a respective antiresonance (AR) dip on the high-frequency side, which are due to the plasmonic lattice periodicity. Similar EOT features have been obtained before in the $T(\omega)$ spectra in the visible[2] and terahertz[10,22] spectral ranges through plasmonic lattices with appropriate lattice constants that match the resonant wavelengths. These EOT resonances have been usually explained by a model that involves SPP coupling to light on the perforated metal surfaces,[2] although other models have also been suggested.[13] A modification of the traditional SPP model[42,43] is described below.

A normally incident light impinging on a smooth metallic surface cannot excite SPP excitations, as these excitations

TABLE I. The antiresonant SPP modes in the $T(\omega)$ spectrum associated with the two interfaces of the perforated Al film, namely, Al/Si and Al/air. The calculated AR frequencies were obtained using Eq. (3) and ε_d from tables. The uncertainties in the values of the experimental AR frequencies are also given.

Interface	SPP mode	AR expt. frequencies (cm^{-1})	AR calc. frequencies (cm^{-1})
Al/Si	(1, 0)	756 (±5)	722
	(1, 1)	1073 (±15)	1021
	(2, 0)	1560 (±50)	1445
	(2, 2)	2150 (±50)	2045
Al/air	(1, 0)	2600 (±50)	2500

can exist only in the transverse magnetic mode on such a metallic surface.[1] However, the periodically spaced holes on the metallic surface allow grating coupling between the incident light and SPP excitations on the two film interfaces. The conservation of quasimomentum in this case is usually written as[2]

$$\vec{k}_{\mathrm{sp}} = \vec{k}_x \pm m\vec{u}_x \pm n\vec{u}_y, \tag{1}$$

where $|\vec{k}_x| = (2\pi/\lambda)\sin\theta$ is the component of the incident light wave vector in the plane of the hole array, and $\vec{u}_x$ and $\vec{u}_y$ are the primitive reciprocal lattice vectors. For a square lattice, we have $|\vec{u}_x| = |\vec{u}_y| = 2\pi/a_0$, where a_0 is the lattice constant of the hole array structure and m, n are integers. From the conservation of energy, we get for the SPP wave vector, k_{spp} on a smooth metallic film,[1]

$$|\vec{k}_{spp}| = \frac{\omega}{c}\left[\frac{\varepsilon_m(\omega)\varepsilon_d}{\varepsilon_m(\omega)+\varepsilon_d}\right]^{1/2}, \tag{2}$$

where $\varepsilon_m(\omega)$ and ε_d are the dielectric constants (mainly the real components) of the metal film and substrates; in our case, Si (with $\varepsilon_d \cong 12$) and air (with $\varepsilon_d = 1$).

At a normal incidence and for $\varepsilon_m \gg \varepsilon_d$, Eqs. (1) and (2) can be reduced to obtain the wavelengths $\lambda_{\min}$ of the ARs in $T(\omega)$ as follows:

$$\lambda_{\min} = \frac{a_0}{\sqrt{m^2+n^2}}\sqrt{\varepsilon_d}. \tag{3}$$

Using this model, the ARs in $T(\omega)$ can be assigned to SPP modes with specific n, m integer parameters associated with the two interfaces,[22] as seen in Fig. 1. The four AR modes (or Wood's anomalies[2,10]) for the Al/Si interface and the single mode for the Al/air interface are summarized in Table I and compared with the theoretical values based on Eq. (3), where ε_d for Si was taken from known literature tables. The agreement between the experimental and theoretical $\lambda_{\min}$ values is remarkable, showing that this SPP model works very well in the MIR range, but for the AR frequencies rather than the resonant peaks in $T(\omega)$ (Ref. 22); this is in contrast to the EOT bands in the visible range, where the SPP attenuation has to be taken into account. Nevertheless, we believe that in order to assign the resonant EOT peaks in $T(\omega)$ and get further insight into the nature of the SPP excitations on a perforated metallic film, one must use the *actual* form of $\varepsilon_m(\omega)$, as opposed to using the metallic dielectric function from a standard database of an unpatterned bulk metal.

We recently proposed to determine the complex "effective" dielectric constant, $\varepsilon_m(\omega)$ for perforated metallic films using an "effective plasma frequency" model,[42,43] and adopt this model here. The dielectric function $\varepsilon_m(\omega)$ used in our calculation was in the following form:

$$\varepsilon_m(\omega) = \varepsilon_\infty\left[1 - \left(\frac{\tilde{\omega}_p^{\,2}}{\omega^2 + i\gamma\omega}\right) + \sum_j \left(\frac{\omega_{L_j}^{\,2} - \omega^2}{\omega_{T_j}^{\,2} - \omega^2 - i\gamma_j\omega}\right)\right], \tag{4}$$

where ε_∞ is the high-frequency dielectric constant, $\tilde{\omega}_p$ is the effective plasma frequency related with the individual, uncorrelated holes, ω_T corresponds to the frequency minima (or ARs) in $T(\omega)$, ω_L is an effective "longitudinal frequency" for the resonant mode that is used here to determine its oscillator strength, S_j (or Rabi frequency) in $\varepsilon_m(\omega)$, which are given by $S_j = (\omega_L/\omega_T)^2 - 1$, and γ_j corresponds to the respective damping constant. Equation (4) has both plasmon (first two terms) and resonant mode (third term) characteristics. The effective plasma term comes from the uncorrelated holes in the perforated metal that does not contain resonances; in fact, it fits well the broad band enhanced transmission in $T(\omega)$ that starts at ~400 cm^{-1}. In contrast, the "resonant mode" term in Eq. (4) is related to the structure factor (or periodicity) of the underlying hole arrays,[22] where ω_{Tj} are the AR frequencies. In the case of zero damping and flat "plasmon response," the term describing the resonant mode characteristics leads to a modified Lyddane-Sachs-Teller (LST) relation.[45] Equation (4) is a generalization of the plasma dielectric function (first two terms) and a LST-type dielectric function $\varepsilon_{LST}(\omega)$ [last term in Eq. (4)], which was used before for describing the optical properties of doped polar semiconductors.[46–48] At temperatures higher than the "impurity freeze-out temperature," such a dielectric response contains a plasma term due to the free carriers released by the dopant impurities, in addition to polar phonons with longitudinal optical and transverse optical modes given by ω_L and ω_T, respectively.

The optical transmission spectrum was calculated using $\varepsilon_m(\omega)$ from Eq. (4) and fitted to the experimental spectrum using a least squares fitting procedure. In the fitting, the ω_T parameters were fixed at the AR frequencies and were taken directly from the experimental $T(\omega)$ spectrum, whereas the plasma parameters $\tilde{\omega}_p$ and γ were fit to the broad continuous transmission band in the spectrum. The other parameters such as ε_∞ and the respective ω_L and γ_j for the individual resonant modes were left free. We focused our attention to the two lowest frequency resonant modes, namely, (1, 0) and (1, 1) SPP modes associated with the Al/Si interface, since they are close to the frequency of the maximum in the thermal emission spectrum obtained at moderately high metal heating temperature. Therefore, in the fitting procedure, we only use these two resonant modes, whereas the contribution to $\varepsilon_m(\omega)$ of the other resonant modes at higher frequencies

TABLE II. The best fit parameters for the calculated $T(\omega)$ spectrum of the Al perforated film [Fig. 3(a)] using the effective dielectric function $\varepsilon_m(\omega)$ calculated using Eq. (4) with two resonant modes.

ε_∞	$\tilde{\omega}_p$ (Hz)	γ (Hz)	ω_{L1} (Hz)	ω_{L2} (Hz)	γ_1 (Hz)	γ_2 (Hz)
3.1	24.6×10^{14}	10.1×10^{14}	12.5×10^{14}	15.4×10^{14}	17.6×10^{12}	39.7×10^{12}

was embedded in the ε_∞ parameter. The calculated $T(\omega)$ spectrum based on the "best fit" parameters given in Table II is shown in Fig. 3 in comparison with the experimental $T(\omega)$. The good agreement obtained between the two $T(\omega)$ spectra validates the model for $\varepsilon_m(\omega)$ used here. Also, the real $\varepsilon_m'(\omega)$ and imaginary $\varepsilon_m''(\omega)$ components of the dielectric spectrum calculated based on the best fit parameters are shown in Fig. 3, inset. It is seen that for each resonant mode, $\varepsilon_m''(\omega)$ shows a narrow maximum at a frequency that corresponds to the middle of the resonant feature in $\varepsilon_m'(\omega)$. This response comes from the well-known Kramers-Kronig relation between the real and imaginary $\varepsilon_m(\omega)$ components and thus validates our calculation method.

In addition, we also calculated the absorption spectrum $\alpha(\omega)$ of the hole array structure from the obtained dielectric function with the "best fit parameters" using the expression $\alpha=\omega\,\mathrm{Im}[n(\omega)]/c$, where $\mathrm{Im}(n)$ is the imaginary component of the refractive index, which was calculated from the fitted $\varepsilon_m(\omega)$ spectrum above, and c is the speed of light. The obtained $\alpha(\omega)$ spectrum is plotted together with $T(\omega)$ in Fig. 3(b). It is apparent that the resonant contributions to $\alpha(\omega)$ are opposite compared with those in $T(\omega)$. $\alpha(\omega)$ shows *maxima* at the AR frequencies and *minima* at the EOT peak frequencies in $T(\omega)$. This is in contrast to the situation in the visible range, where it was shown[12] that $\alpha(\omega)$ and $T(\omega)$ show similar resonant features, where maxima in $\alpha(\omega)$ corresponded with maxima in the EOT spectrum.

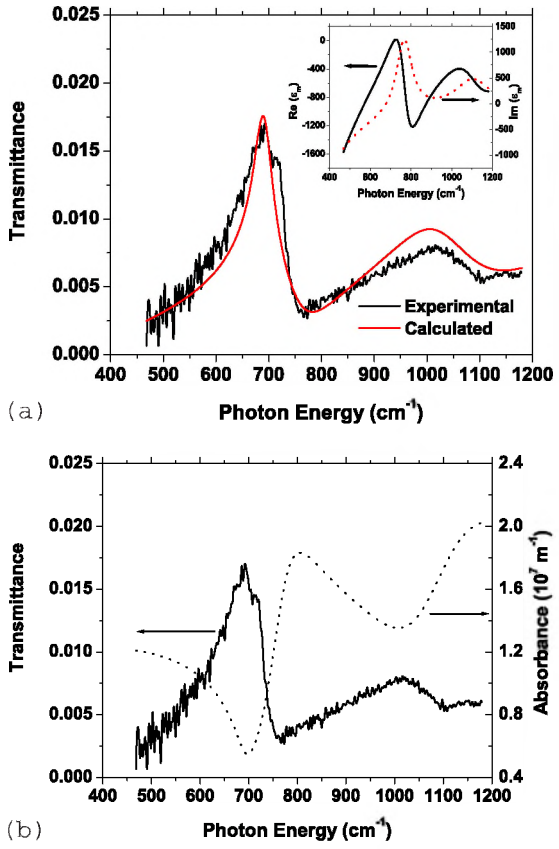

FIG. 3. (Color online) (a) A comparison between the experimental and calculated transmission spectra using $\varepsilon_m(\omega)$ calculated via Eq. (4) with the best fitting parameters given in Table II. The inset shows the corresponding calculated real and imaginary components of the dielectric response $\varepsilon_m(\omega)$. (b) The calculated absorption spectrum $\alpha(\omega)$ compared with the experimental transmission spectrum $T(\omega)$.

B. Thermal emission spectra

In order to eliminate the system spectral response and any optical loss during the thermal emission measurements, we computed the hole array normalized emissivity spectrum $E(\omega)$ from the directly measured emission spectrum $E_H(\omega)$. $E(\omega)$ was obtained by dividing the hole array emission spectrum by the emission spectrum $E_M(\omega)$ of an unpatterned metal film having identical thickness and measured at *the same heated metal temperature*. The procedure is described below,

$$E_H(\omega) = S(\omega)\xi(\omega)D(\omega),$$

$$E_M(\omega) = F(\omega)\xi(\omega)D(\omega),$$

$$E(\omega) = \frac{E_H(\omega)}{E_M(\omega)}. \tag{5}$$

In Eq. (5), $\xi(\omega)$ represents the optical propagation loss as thermal emission passes through the spectrometer and reaches the photodetector, and $D(\omega)$ represents the combined optical window and photodetector and/or beam-splitter spectral response. We note that the Planck distribution function $K(\omega,T)$ for blackbody radiation emission, which is presumably the same for the heated perforated and unperforated films at the same temperature, is readily taken into account by this procedure. Consequently, it is no longer a factor in the analysis below.

The normalized emissivity spectrum $E(\omega)$ of the Al hole array obtained following the procedure described in Eq. (5) is shown in Fig. 4(a). $E(\omega)$ contains several emission bands, but the modification of the perforated film emissivity spectrum compared to that of an unperforated film is quite small. This is apparent in Fig. 4(a), where the modifications of the emissivity spectrum are seen to be around the value of 1. In addition, none of the emissivity bands corresponds to resonances found in the absorption spectrum [Fig. 4(b)]. In fact,

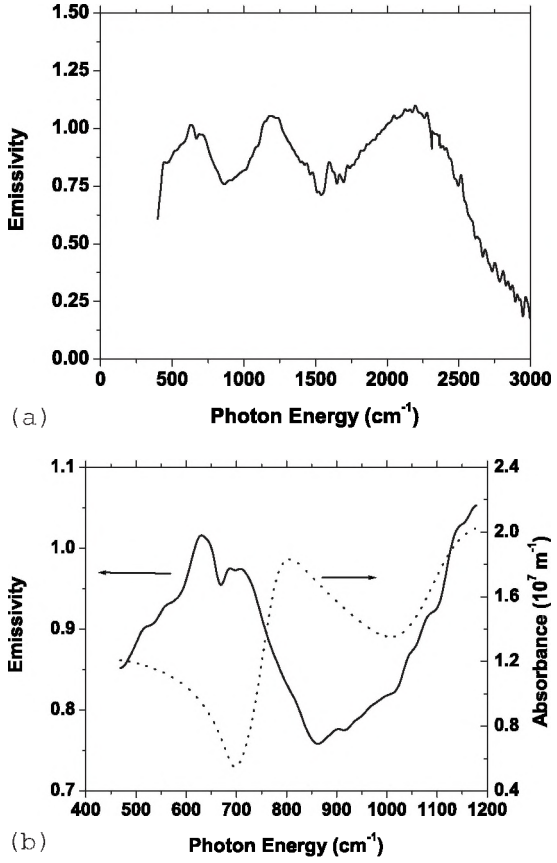

FIG. 4. (a) The normalized emissivity spectrum $E(\omega)$ of the plasmonic lattice sample using the procedure described in Eq. (5). (b) Comparison between the $E(\omega)$ and calculated $\alpha(\omega)$ spectra.

$E(\omega)$ better fits $T(\omega)$ rather than the $\alpha(\omega)$ spectrum (see Fig. 1). For example, the lowest peak in $E(\omega)$ is observed at about 650 cm^{-1}, close to that of the lowest peak in $T(\omega)$. However, this emissivity band is out of phase (opposite) from that in $\alpha(\omega)$, which shows a dip rather than a peak at $\sim$700 cm^{-1}. This is close to the $E(\omega)$ peak rather than a dip.

In order to ensure that the transmission and absorption spectra of the sample are considered at the correct temperature, we measured $T(\omega)$ of the hole array also at elevated temperature (Fig. 5). It is seen that $T(\omega)$ does not change much with the temperature. This validates the conclusion that $E(\omega)$ more closely resembles $T(\omega)$, even when the high sample temperature needed for the radiation emission is taken into account.

From Kirchhoff's law, the emission spectrum of a body (or a surface) in thermal equilibrium is equal to the absorbance $A(\omega)$ weighted by the blackbody distribution spectrum $K(\omega,T)$ at the temperature T of the measurement, such that[49]

$$E(\omega,T) = A(\omega)K(\omega,T), \tag{6}$$

where $K(\omega,T)$ is the well-known Planck distribution given by the expression

$$K(\omega,T) = \frac{\hbar\omega^3}{\pi^2 c^3}\left(\frac{\hbar\omega}{e^{\hbar\omega/k_B T}-1}\right), \tag{7}$$

where h is the Planck constant and k is the Boltzmann constant. In Eq. (6), the effects of the photonic DOS of such a

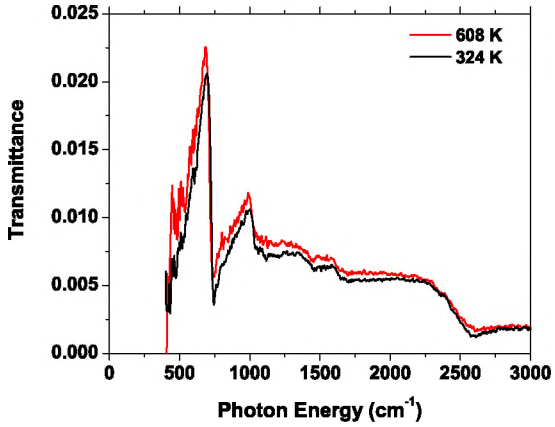

FIG. 5. (Color online) Transmission spectra of the Si-supported Al hole array measured at normal incidence at temperatures of 324 and 608 K.

complex structure are fully captured through $A(\omega)$. Since $E(\omega)$ does not resemble $\alpha(\omega)$, there seems to be a violation of Kirchhoff's law given in Eq. (6). The apparent violation of Kirchhoff's law may arise from the fact that the response of our system is not in thermodynamic equilibrium.[40] Specifically, there is a temperature gradient across the sample film that is maintained at steady state conditions established by the heat flow, and there is lack of thermal equilibrium with the sample surrounding. However, the fact that $\alpha(\omega)$ differs from $E(\omega)$ while $T(\omega)$ and $E(\omega)$ are closely related is quite suggestive.

We thus conclude from the similarity between the emissivity and transmission spectra that the hole array structure behaves as a *radiation filter*, where the emissivity is suppressed outside the EOT bands. In order to verify this hypothesis, we calculated from the measured spectra an effective "transfer function," $G(\omega)$ using the ratio between the obtained $E(\omega)$ and $\alpha(\omega)$ spectra (see Fig. 6). The close similarity between $G(\omega)$ and $T(\omega)$ measured at the same temperature supports our conclusion. The emissivity spectral characteristics of the hole array are indeed affected compared

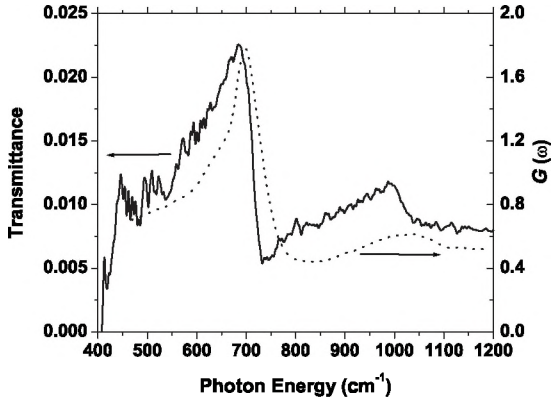

FIG. 6. The transfer function $G(\omega)$ (dashed line, right scale) calculated from the emissivity and absorption spectra shown in Fig. 4(b), compared with the measured $T(\omega)$ spectrum at the same temperature of the thermal emission experiment (full line, left scale).

to an unperforated film but primarily through a modification induced by the transmission spectrum. Therefore, we conjecture that in perforated metallic films, there exists *weak coupling* between the MIR photon DOS in the metal and the SPP excitations on the metal interfaces.

The obtained modified emission $G(\omega)$ and its similarity with $T(\omega)$ that are seen here are analogous to the photoluminescence (PL) spectrum of a light source or chromophores embedded inside a *weak* 3D photonic crystal, which has stop bands but lacks a complete photonic band gap. In such photonic crystals, the refraction index contrast between the constituent materials is not large enough to considerably alter the photon DOS. The PL spectra in weak 3D photonic crystal opals infiltrated with dye molecules and π-conjugated polymers were measured before,[44] where stop bands in the emission spectra were clearly observed. It was indeed concluded that due to the weak influence of the underlying photonic crystal over the photonic DOS, the modified PL spectrum was mainly induced by the transmission through the opal rather than modification induced by the photon DOS in the photonic crystal. In our case too, the SPP excitations on the metal interfaces do not considerably alter the MIR photon DOS of the thermal radiating element but mainly act as a radiation filter[50] to the slightly modified emissivity spectrum. It is worth noting, however, that the ability of a *stronger* 3D photonic crystal to modify the absorption and thermal emission may enhance the performance of lasers, detectors,[51] solar cells, and infrared thermal image control.[52] These applications may therefore justify further investigations of thermal emission from metamaterials.

IV. CONCLUSIONS

In conclusion, we measured the extraordinary optical transmission spectrum through a subwavelength hole array on an optically opaque Al film in the MIR spectral range. The transmission spectrum contains both resonances and antiresonances superposed on a smooth continuous band and is well explained using a modification of the standard model of light coupling to SPP excitations on the two film interfaces.[2] The effective dielectric response function of the plasmonic lattice was calculated using a generalized form of a LST-type dielectric function that describes the resonant modes in the presence of an effective plasma frequency due to the individual holes. From the fitted dielectric response, we calculated the absorption spectrum and found that it contains optical features that are opposite in phase to the resonant bands in transmission, in contrast to the obtained spectra in the visible spectral range.

The thermal emission spectrum measured from the hole array at elevated heated temperature was found to have a close correspondence with the transmission spectrum, whereas the calculated absorption spectrum differed significantly. Further extraction of the effective transfer function and a comparison with the transmission spectrum led us to conclude that such hole array structures behave as radiation filters by suppressing the emission outside their transmission bands. We thus conclude that plasmonic lattices cannot strongly modify the emission spectrum, in contrast to what was expected previously.

ACKNOWLEDGMENTS

We thank M. Delong for help with the FTIR measurements. This work was supported in part by the ARO and the SYNERGY program at the University of Utah.

*val@physics.utah.edu

†Present address: Department of Electrical and Electronic Engineering, Mie University, 1577 Kurimamachiya, Tsu, Mie 514-8507, Japan.

[1] H. Raether, in *Surface Plasmons on Smooth and Rough Surfaces and on Gratings* (Springer-Verlag, Berlin, 1988).

[2] T. W. Ebbesen, H. J. Lezec, H. F. Gaemi, T. Thio, and P. A. Wolff, Nature (London) **391**, 667 (1998).

[3] H. F. Ghaemi, T. Thio, D. E. Grupp, T. W. Ebbesen, and H. J. Lezec, Phys. Rev. B **58**, 6779 (1998).

[4] T. J. Kim, T. Thio, T. W. Ebbesen, D. E. Grupp, and H. J. Lezec, Opt. Lett. **24**, 256 (1999).

[5] M. M. J. Treacy, Appl. Phys. Lett. **75**, 606 (1999).

[6] L. Martin-Moreno, F. J. Garcia-Vidal, H. J. Lezec, K. M. Pellerin, T. Thio, J. B. Pendry, and T. W. Ebbesen, Phys. Rev. Lett. **86**, 1114 (2001).

[7] A. Krishnan, T. Thio, T. J. Kim, H. J. Lezec, T. W. Ebbesen, P. A. Wolff, J. Pendry, L. Martin-Moreno, and F. J. Garcia-Vidal, Opt. Commun. **200**, 1 (2001).

[8] W. L. Barnes, A. Dereux, and T. W. Ebbesen, Nature (London) **424**, 824 (2003).

[9] J. Gomez Rivas, C. Schotsch, P. Haring Bolivar, and H. Kurz, Phys. Rev. B **68**, 201306(R) (2003).

[10] M. Sarrazin, J. P. Vigneron, and J. M. Vigoureux, Phys. Rev. B **67**, 085415 (2003).

[11] W. L. Barnes, W. A. Murray, J. Dintinger, E. Devaux, and T. W. Ebbesen, Phys. Rev. Lett. **92**, 107401 (2004).

[12] K. J. Klein Koerkamp, S. Enoch, F. B. Segerink, N. F. van Hulst, and L. Kuipers, Phys. Rev. Lett. **92**, 183901 (2004).

[13] H. J. Lezec and T. Thio, Opt. Express **12**, 3629 (2004).

[14] H. Cao and A. Nahata, Opt. Express **12**, 1004 (2004).

[15] Y. H. Ye and J. Y. Zhang, Appl. Phys. Lett. **84**, 2977 (2004).

[16] P. Lalanne, J. C. Rodier, and J. P. Hugonin, J. Opt. A, Pure Appl. Opt. **7**, 422 (2005).

[17] F. J. Garcia de Abajo, J. J. Saenz, I. Campillo, and J. S. Dolado, Opt. Express **14**, 7 (2006).

[18] A. Agrawal and A. Nahata, Opt. Express **14**, 1973 (2006).

[19] G. Gay, O. Alloschery, B. Viaris de Lesegno, C. O'Dwyer, J. Weiner, and H. J. Lezec, Nat. Phys. **2**, 262 (2006).

[20] M. Sun, J. Tian, Z.-Y. Li, B.-Y. Cheng, D.-Z. Zhang, A.-Z. Jin, and H.-F. Yang, Chin. Phys. Lett. **23**, 486 (2006).

[21] F. Przybilla, C. Genet, and T. W. Ebessen, Appl. Phys. Lett. **89**,

121115 (2006).
[22] T. Matsui, A. Agrawal, A. Nahata, and Z. V. Vardeny, Nature (London) **446**, 517 (2007).
[23] N. Papasimakis, V. A. Fedotov, F. J. Garcia de Abajo, A. S. Schwanecke, and N. I. Zheludev, arXiv:0704.2552v1 (unpublished).
[24] J. Bravo-Abado, A. I. Fernandez-Dominquez, F. J. Garcia-Vidal, and L. Martin-Moreno, report, 2007 (unpublished).
[25] Y.-J. Bao, B. Zhang, Z. Wu, J.-W. Si, M. Wang, R.-W. Peng, X. Lu, J. Shao, Z.-F. Li, X.-P. Hao, and N.-B. Ming, Appl. Phys. Lett. **90**, 251914 (2007).
[26] T. Neumann, M.-L. Johanson, D. Kambhampati, and W. Knoll, Adv. Funct. Mater. **12**, 575 (2002).
[27] P. A. Hobson, S. Wedge, J. A. E. Wasey, I. Sage, and W. L. Barnes, Adv. Mater. (Weinheim, Ger.) **14**, 1393 (2002).
[28] C. Liu, V. Kamaev, and Z. V. Vardeny, Appl. Phys. Lett. **86**, 143501 (2005).
[29] R. Ziblat, V. Lirtsman, D. Davidov, and B. Aroeti, Biophys. J. **90**, 1 (2006).
[30] J. G. Fleming, S. Y. Lin, I. El-Kady, R. Biswas, and K. M. Ho, Nature (London) **417**, 52 (2002).
[31] C. M. Cornelius and J. P. Dowling, Phys. Rev. A **59**, 4736 (1999).
[32] S. Y. Lin, J. G. Fleming, E. Chow, J. Bur, K. K. Choi, and A. Goldberg, Phys. Rev. B **62**, R2243 (2000).
[33] M. U. Pralle, N. Moelders, M. P. McNeal, I. Puscasu, A. C. Greenwald, J. T. Daly, E. A. Johnson, T. George, D. S. Choi, I. El-Kady, and R. Biswas, Appl. Phys. Lett. **81**, 4685 (2002).
[34] S. Y. Lin, J. Moreno, and J. G. Fleming, Appl. Phys. Lett. **83**, 380 (2003).
[35] S. Y. Lin, J. G. Fleming, and I. El-Kady, Appl. Phys. Lett. **83**, 593 (2003).
[36] C. Luo, A. Narayanaswamy, G. Chen, and J. D. Joannopoulos, Phys. Rev. Lett. **93**, 213905 (2004).
[37] S. Y. Lin, J. G. Fleming, and J. Moreno, Appl. Phys. Lett. **84**, 1999 (2004).
[38] I. El-Kady, W. W. Chow, and J. G. Fleming, Phys. Rev. B **72**, 195110 (2005).
[39] T. Trupke, P. Wurfel, and M. A. Green, Appl. Phys. Lett. **84**, 1997 (2004); S. Y. Lin, J. Morebno, and J. G. Fleming, *ibid.* **84**, 1999 (2004).
[40] J. G. Fleming, Appl. Phys. Lett. **86**, 249902 (2005).
[41] I. Puscasu, M. Pralle, M. McNeal, J. Daly, A. Greenwald, E. Johnson, R. Biswas, and C. G. Ding, J. Appl. Phys. **98**, 013531 (2005).
[42] J. B. Pendry, L. Martin-Moreno, and F. J. Garcia-Vidal, Science **305**, 847 (2004); F. J. Garcia-Vidal, L. Martin-Moreno, and J. B. Pendry, J. Opt. A, Pure Appl. Opt. **7**, S97 (2005).
[43] A. Agrawal, Z. V. Vardeny, and A. Nahata (unpublished).
[44] N. Eradat, M. Wohlgenannt, Z. V. Vardeny, A. A. Zakhidov, and R. H. Baughman, Synth. Met. **116**, 509 (2001).
[45] R. H. Lyddane, R. G. Sachs, and E. Teller, Phys. Rev. **59**, 673 (1941); E. L. Albuquerque and M. G. Cottam, *Polaritons in Periodic and Quasiperiodic Structures* (Elsevier, Amsterdam, 2004), Chap. 1, p. 3.
[46] A. Mooradian and G. B. Wright, Solid State Commun. **4**, 431 (1966).
[47] I. F. Chang and S. S. Mitra, Phys. Rev. **172**, 924 (1968).
[48] K. J. Nash, M. S. Skolnick, and S. J. Bass, Semicond. Sci. Technol. **2**, 329 (1987).
[49] E. M. Lifshitz, L. D. Landau, and L. P. Pitaevskii, *Electrodynamics of Continuous Media* (Academic, New York, 1984).
[50] S. G. Romanov, T. Maka, C. M. Sotomayor Torres, M. Müller, and R. Zentel, Appl. Phys. Lett. **75**, 1057 (1999); E. P. Petrov, V. N. Bogomolov, I. I. Kalosha, and S. V. Gaponenko, Phys. Rev. Lett. **81**, 77 (1998).
[51] B. E. A. Saleh and M. C. Teich, *Fundamentals of Photonics* (Wiley, New York, 1991), Chap. 17, p. 648.
[52] F. K. Hopkins, Opt. Photonics News **9**, 32 (1998).